Interstitial iron impurities at cores of dissociated dislocations in silicon

Benedikt Ziebarth,[1,2,*] Matous Mrovec,[1,†] Christian Elsässer,[1] and Peter Gumbsch[1,2]
[1]*Fraunhofer-Institut für Werkstoffmechanik IWM, Wöhlerstrasse 11, 79108 Freiburg, Germany*
[2]*Institut für Angewandte Materialien (IAM), Karlsruher Institut für Technologie, Engelbert-Arnold-Strasse 4, 76131 Karlsruhe, Germany*
(Received 28 September 2015; revised manuscript received 28 October 2015; published 24 November 2015)

Dislocations play an important role in semiconductor devices made of crystalline silicon (Si). They are known to be strongly performance-limiting defects in solar cell applications, since they act as preferred segregation sites for metallic impurities. In this work we investigate the segregation of iron (Fe) to the cores of the 30° and 90° partial dislocations in Si using atomistic calculations based on first-principles density functional theory. Our simulations show that interstitial Fe impurities segregate readily to all investigated cores and the driving force for the segregation increases with impurity concentration. Moreover, our analysis of the electronic structure reveals the existence of deep defect levels within the band gap that can be related to experimental observations by deep-level transient spectroscopy.

DOI: 10.1103/PhysRevB.92.195308 PACS number(s): 71.15.Mb, 61.72.Lk, 88.40.jj, 64.75.Qr

I. INTRODUCTION

Dislocations can strongly influence the performance and reliability of electronic devices made of silicon (Si). For instance, in multicrystalline silicon (mc-Si) solar cell dislocations act as recombination centers that lower the charge carrier lifetime and diffusion length. This recombination is strongly enhanced by metallic impurities that segregate at dislocation cores and introduce deep defect levels in the band gap [1,2]. Among metallic impurities, iron (Fe) is known to have a particularly strong detrimental effect on the efficiency of mc-Si based devices [3]. A direct correlation between interstitial Fe concentration and dislocation density [4] has indicated that there is a likely preferential segregation of Fe at dislocation cores. This has been further supported by transmission electron microscopy observations of Fe-decorated dislocations in SiGe/Si heterostructures [5].

Despite its importance there are no systematic theoretical studies of the interaction between interstitial Fe impurities and dislocation cores in Si. Most computational studies on dislocations in Si have focused on the atomic arrangement [6–8], thermodynamics [6,9], and kinetics [6,10,11] of clean dislocation cores. The segregation of impurities at dislocations has been investigated only for a few elements, including hydrogen [12,13], arsenic [14,15], and copper (Cu) [16]. Since the first two elements are not metallic, they are expected to behave differently than Fe. For Cu, a late transition metal, the calculations were limited to substitutional Cu defects only [16].

The Fe impurities are known to occupy tetrahedral interstitial sites in the diamond-type crystal structure of bulk Si [17]. In p-type doped Si the Fe interstitial is positively charged (Fe^{+}) while in n-type or not doped Si it remains uncharged (Fe^{0}) [17,18]. The presence of the Fe impurity leads to an emergence of a deep donor level at 0.4 eV above the valence band edge of bulk Si which causes the charge carriers (electrons and holes) to recombine easily [17].

In this work we present a computational study based on first-principles density functional theory (DFT) of interactions between interstitial Fe impurities and dislocation cores in Si. This paper builds on our preceding studies of Fe segregation at interfaces [19] and Fe segregation and diffusion in the long-ranged elastic strain fields of dislocations in Si [20]. The latter showed that the elastic distortions of the lattice around dislocations do not give rise to any preferential segregation of Fe impurities. However, as will be shown in this paper, the situation is markedly different at dislocation cores whose local atomic structures are significantly more distorted.

The paper is organized as follows: In Sec. II the computational setup is described, the structural models for the dislocation cores are presented in Sec. III, the results of the calculations on the segregation of Fe impurities are given in Sec. IV, and the outcomes are discussed and analyzed in Sec. V.

II. COMPUTATIONAL METHODS

DFT calculations have been carried out using the Quantum Espresso PWscf code [21], which uses a plane-wave basis to express the wave functions of the valence electrons. Interactions of ionic cores and valence electrons are described by ultrasoft pseudopotentials. The PBE generalized gradient approximation was used for exchange correlation [22,23]. All calculations in which Fe was involved were spin polarized. Energy cutoffs of 35 and 350 Ry for the plane-wave basis and electron-density representation, respectively, were found to yield converged results. For the calculations of total energies and forces only the Γ point in the Brillouin zone was used. Densities of states were calculated using a $2\times2\times2$ k-point mesh. Atom positions were relaxed until the remaining forces acting on the atoms were less than 10^{-3} eV/Å. Calculations have been managed using the atomic simulation environment (ASE) [24].

III. ATOMISTIC MODELS OF DISLOCATIONS

In the diamond structure of Si, perfect dislocations have Burgers vectors **b** equal to $a/2\langle110\rangle$, where $a = 5.47$ Å is the equilibrium cubic lattice constant of Si as obtained

*Benedikt.Ziebarth@gmail.com
†Matous.Mrovec@iwm.fraunhofer.de

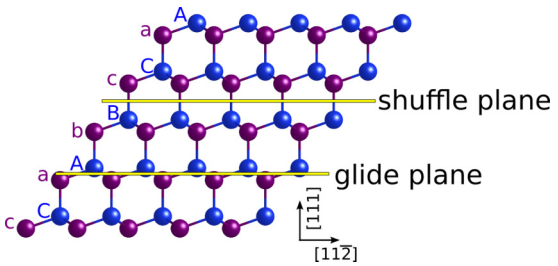

FIG. 1. (Color online) Stacking of the {111} planes in the Si diamond structure. Blue and purple spheres mark the Si atoms of the two fcc sublattices.

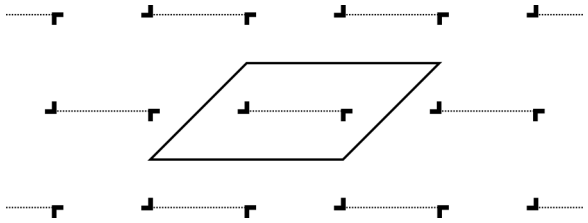

FIG. 2. Schematic view of the periodic arrangement of dislocations. The supercell contains a dislocation dipole of partial dislocations which forms a lattice of dislocation quadrupoles when the supercell is periodically repeated. The dashed lines correspond to the stacking faults connecting the partial dislocations.

from our DFT-PBE calculations. Experimental observations have revealed that there are only two types of perfect dislocations in Si—a pure screw dislocation and a 60° mixed dislocation [6]. Both dislocations glide on the close-packed {111} planes. Since the diamond structure is build from two face-centered-cubic (fcc) sublattices, there is an alternating stacking ... AaBbCcAaBbCc ... of the {111} planes, where the layers labeled by uppercase letters belong to one sublattice and the lowercase letters denote layers of the other sublattice (see Fig. 1). These two sets of {111} planes have also two distinct interplanar spacings. The narrowly spaced planes (aA, bB, cC) are called *glide* planes, while the widely spaced planes (Ab, Bc, Ca) are called *shuffle* planes. The dislocation core can be, in principle, located between either of the planes [25,26]. If the core is centered between the glide set of planes, it can dissociate into partial dislocations with Burgers vectors $a/6\langle 211\rangle$ according to [6,26]

$$\frac{a}{2}[1\bar{1}0] \rightarrow \frac{a}{6}[2\bar{1}\bar{1}] + \frac{a}{6}[1\bar{2}1], \tag{1}$$

where the dissociated partial dislocations are connected by an intrinsic stacking fault of very low energy. The perfect screw dislocation dissociates into two 30° partial dislocations, while the 60° dislocation dissociates into one 30° and one 90° partial dislocation [6]. The dissociated dislocations are energetically favorable and have been confirmed by high-resolution transmission electron microscopy [6,27]. These two partial dislocation cores (30° and 90°) were therefore chosen for our study of the interaction with the Fe impurities.

The long-range elastic stress and strain fields of dislocations make it challenging to simulate dislocations using small periodic supercells, which are treatable by electronic structure calculations. In our previous study [20] we investigated the interaction of Fe impurities with the long-range elastic fields of dislocations using a combined atomistic/kinetic Monte Carlo approach. In the present work we can focus on the core region and study the segregation of Fe only close to the dislocation cores. We therefore employ a common supercell geometry with a quadrupole arrangement of dislocations (see Fig. 2). In this periodic arrangement of dislocations, most of the long-range stress and strain fields of the individual partial dislocations are canceled in the region between the dislocation cores [28–32]. A nonrectangular supercell with two dislocations of opposite Burgers vectors is a suitable atomic representation for such a dislocation arrangement. We used supercells containing 512 Si atoms, which were found to be sufficiently large to obtain correct core configurations without any spurious interactions. The thickness of the supercell along the dislocation line amounted to $4a[1\bar{1}0]$ to enable the investigation of different Fe concentrations (see below). In the directions perpendicular to the dislocation line the supercell has the dimensions $4a[11\bar{2}]$ and $8a[111]$.

It is known that both cores can undergo reconstructions along the dislocation line [6]. The unreconstructed and reconstructed configurations of the 30° partial core are shown in Fig. 3. The unreconstructed core of the 30° partial dislocation is not stable and reconstructs spontaneously during relaxation of the supercell [33]. For the partial 90° dislocation, there exist at least two different core configurations, termed as the single period (SP) and the double period (DP) reconstruction, shown in Fig. 4 [9,34]. Both the SP and DP reconstructed cores of the 90° partial dislocation are metastable. We found that the DP core is by about 0.08 eV/Å more stable than the SP core, in agreement with other DFT studies of Benneto *et al.* (0.10 eV/Å) [34] and Valladares *et al.* (0.04 eV/Å) [9].

IV. SEGREGATION OF Fe IMPURITIES AT DISLOCATION CORES

A. Atomic structure and energetics

In the following we focus on the interaction between the interstitial Fe impurities and the two partial dislocation cores. As mentioned in Sec. III, we employed a large supercell with a period of $4a[1\bar{1}0] = 4\boldsymbol{\xi}$, along the direction of the dislocation line $\hat{\boldsymbol{\xi}} = \boldsymbol{\xi}/\xi$, in order to be able to examine to which extent the segregation as well as the core structure are influenced by Fe concentration. Our setup allows us to vary the Fe concentration from 1 to 4 Fe atoms per core in the supercell. The investigated impurity concentrations then correspond to 0.25, 0.5, and 1.0 Fe atom/ξ.

To investigate the energy landscape of Fe inside the dislocation core, we first inserted a single Fe atom at different positions along the dislocation line. Initially, only the position of the Fe atom was relaxed while the positions of the Si atoms were kept fixed. Then the low-energy configurations were selected and full structure optimizations were carried out using the BFGS algorithm [35]. The relaxed Fe positions were then used for the construction of initial supercells containing two or four Fe atoms in the core. These supercells were then also fully relaxed. The most stable configurations of Fe impurities at all investigated dislocation cores are shown in Fig. 5. The

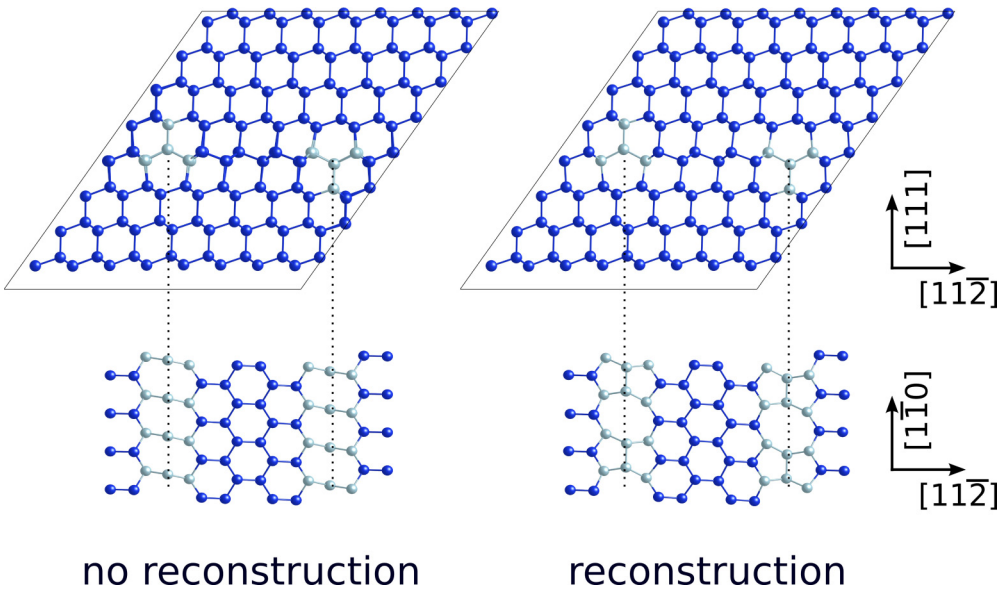

FIG. 3. (Color online) Supercell models of the 30° partial dislocations with different core structures. The upper panels show the dislocations oriented along the dislocation line and the bottom panels show the reconstruction patterns of the dislocations. Blue spheres indicate Si atoms and light blue spheres indicate Si atoms which form the core of the dislocation. The dashed lines are guides to the eyes.

structures of the second and third most stable configurations are displayed in the Supplemental Material [36].

For all configurations, segregation energies were obtained according to

$$E_{\mathrm{Fe}}^{\mathrm{seg}} = \frac{E^{\mathrm{with\ Fe}} - E^{\mathrm{without\ Fe}} - N_{\mathrm{Fe}}\mu_{\mathrm{Fe}}}{N_{\mathrm{Fe}}}, \qquad (2)$$

where $E^{\mathrm{with\ Fe}}/E^{\mathrm{without\ Fe}}$ is the total energy of the Si dislocation supercell with/without an Fe atom, N_{Fe} is the number of Fe atoms in the supercell, and μ_{Fe} is the chemical potential, which is set to the total energy of an interstitial Fe atom in a perfect bulk Si crystal. Note that within this definition a negative segregation-energy value favors segregation while no segregation is expected for a positive value.

The absolute value of the segregation energy (cf. Fig. 5) is largest for the SP and DP reconstructions of the 90° partials and smallest for the reconstructed 30° partial. For all dislocation cores, the segregation energies for impurity concentrations of 0.25 and 0.5 Fe atom/ξ are very similar. This indicates that the interaction energy between the Fe atoms is negligible for these concentrations. In contrast, for the largest concentration of 1 Fe atom/ξ, we observe that the segregation energies decrease significantly, i.e., the segregation becomes more favorable for the weakly attractive DP reconstruction and the 30° partial.

B. Electronic structure analysis

The electronic densities of states (DOS) of the three considered dislocation cores (cf. Fig 5) without and with segregated Fe atoms are displayed in Fig. 6. For comparison, also the DOS for the perfect Si crystal without and with interstitial Fe at a tetrahedral interstitial position is shown. For

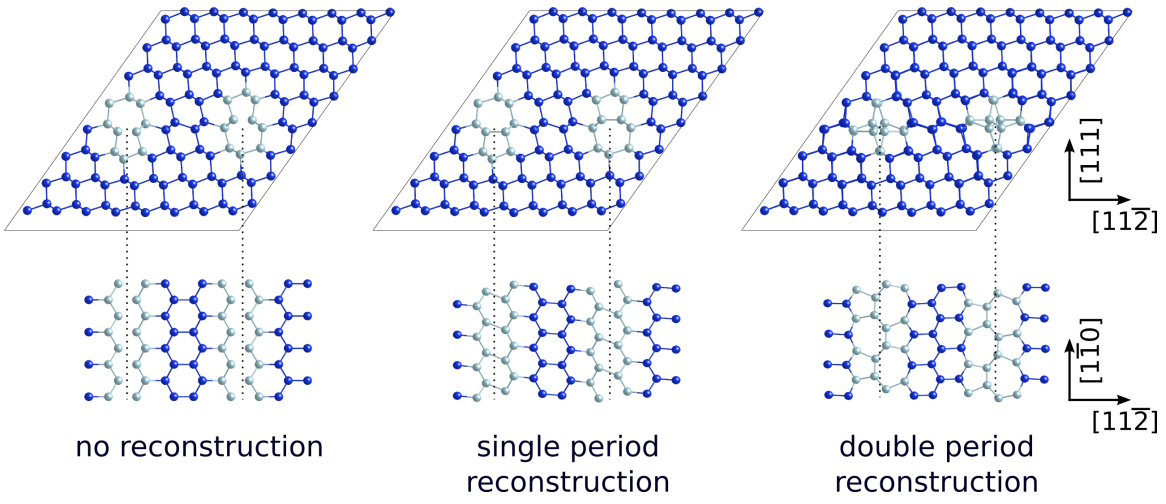

FIG. 4. (Color online) Supercell models of the 90° partial dislocations with different core structures, displayed in the same way as in Fig. 3.

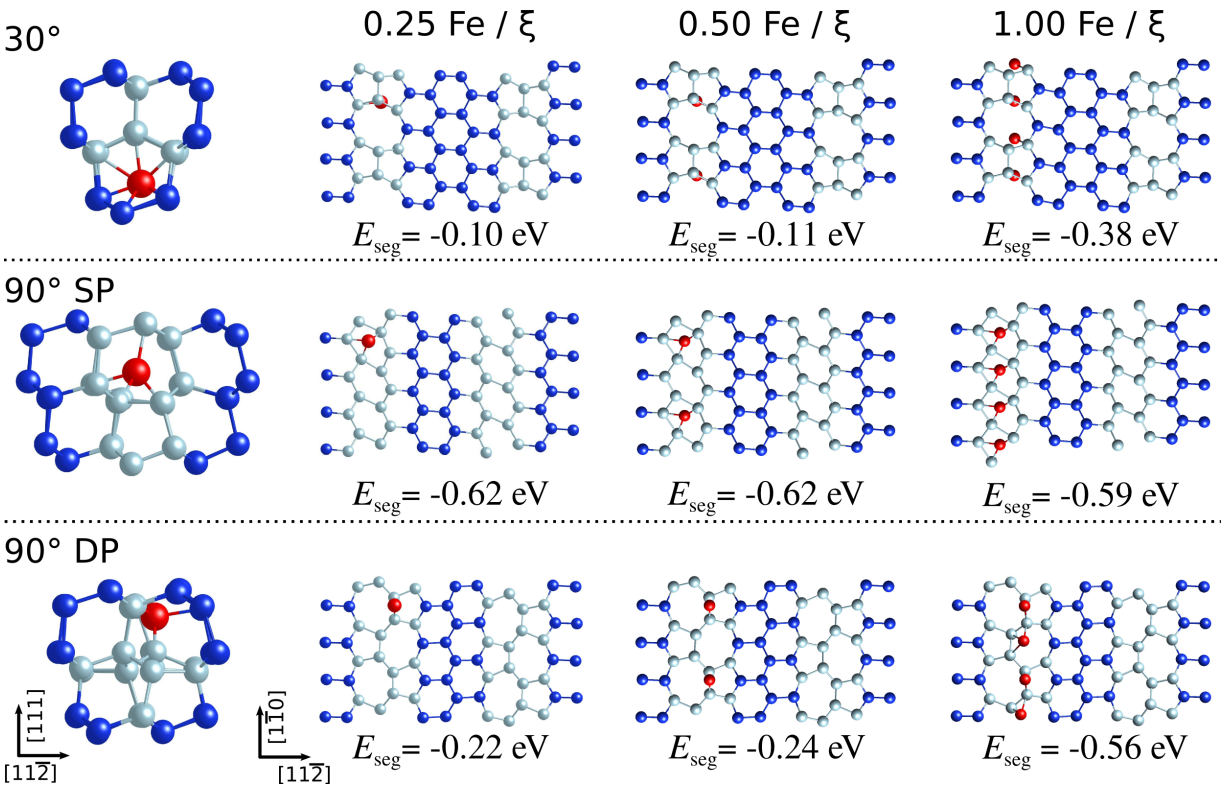

FIG. 5. (Color online) Atomic structures of the most stable configurations of segregated Fe impurities (red spheres) at investigated cores. The left column shows the location of the Fe atom viewed along the dislocation line for a concentration of 0.25 Fe atom/ξ. The other columns show the location of the Fe atoms from a top view for increasing Fe concentrations. Blue spheres indicate Si atoms and light blue atoms indicate Si atoms that correspond to the dislocation cores.

the d states of Fe, projected DOS have been calculated. In Fig. 6 they are displayed as gray-shaded areas. A decomposition of the d states into cubic t_{2g} and e_g contributions is included (red and blue lines, respectively) in Fig. 6. For the interstitial sites at the dislocation cores this decomposition is only approximate since the Si atoms surrounding the Fe interstitial do not have a perfect cubic (octahedral or tetrahedral) symmetry. The orbital directions for the projection were chosen to be same as those for the perfect Si crystal.

In agreement with previous studies [17–19], our calculations yield for interstitial Fe in bulk Si that two electrons are transferred from 4s to 3d states. This leads to a filling of the d states of Fe by eight instead of six electrons per Fe atom. Moreover, the high-spin configuration for the Fe atom is favored such that the spin-up d states are completely filled and the spin-down d states are partially filled by three electrons. The tetrahedral crystal field of the surrounding Si atoms splits the spin-down states into t_{2g} and e_g states. The t_{2g} states are located above the edge of the valence band and correspond to the deep defect states known from several studies [17–19]. The e_g states are shifted to the conduction band and remain unoccupied.

In the case of a clean 30° partial dislocation, the band gap is narrowed but still open. For Fe concentrations of 0.25 and 0.5 Fe atom/ξ, the segregated Fe creates several gap states that cannot be clearly discriminated as t_{2g} and e_g states. While the first peak is still at the same position as the t_{2g} states of Fe in bulk Si, an additional peak appears in the band gap about 0.4 eV higher in energy.

For the clean 90° partial dislocation with SP core, the band gap is closed while with DP core it remains almost the same as in bulk Si. This feature of chemical bonding is likely reflected by the higher energy of the SP core compared to the DP core. The partial d-DOS of segregated Fe for the SP core at the two lower concentrations are similar to that of interstitial Fe in bulk Si, but one of the t_{2g} states is shifted to a lower energy. The local electronic structure of the DP core is similar to that of the 30° partial.

For all three dislocation cores, the highest concentration of 1 Fe atom/ξ induces much more significant changes in the electronic structure as the atomlike d states start to broaden to a crystal-like d band. For the case of the DP core of the 90° dislocation, the system even becomes spin unpolarized and thus qualitatively very different from those with the lower impurity concentrations.

V. DISCUSSION AND CONCLUSION

We investigated the segregation of interstitial Fe atoms at the three most relevant core structures of partial dislocations in Si. In all considered configurations, the Fe interstitials are attracted to the dislocation cores. The segregation energies do not depend on the impurity concentration if it remains lower than 0.5 Fe atom/ξ, i.e., the Fe atoms are separated by at least 2ξ and are uniformly distributed along the dislocation line. For these concentrations, the system can be considered to be in the dilute limit. This is supported by the calculations of the electronic densities of states which look almost identical

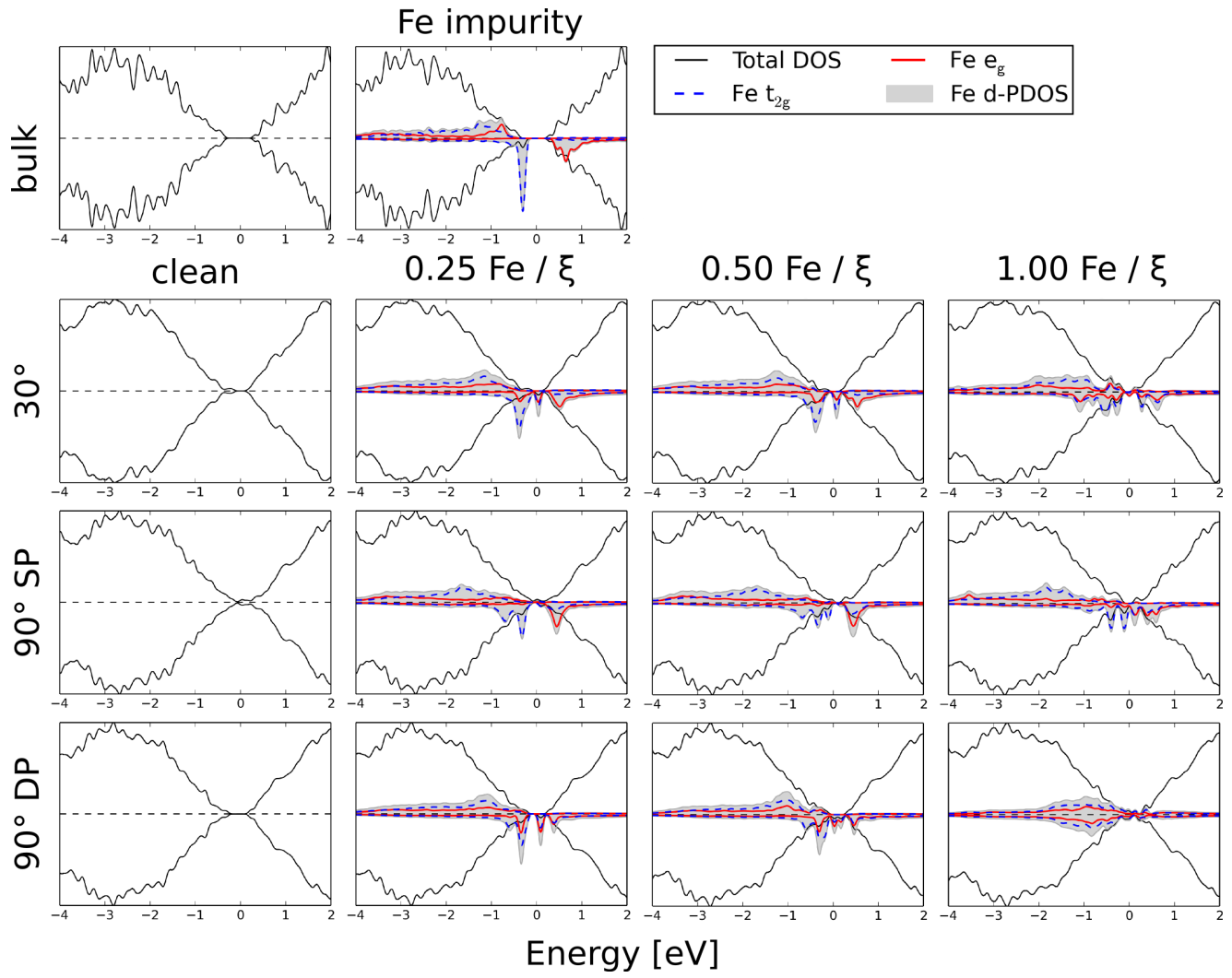

FIG. 6. (Color online) Total and projected electronic densities of states for the bulk crystal and the 30° DP, 90° SP, and 90° DP dislocation cores without and with segregated interstitial Fe for different impurity concentrations. For clarity, the projected densities of states of the states of Fe are scaled.

for the impurity concentration of 0.25 and 0.5 atom/ξ (cf. Fig. 6). In the dilute limit a rather small segregation energy of about -0.10 eV is found for the 30° partial dislocation. For the 90° partial dislocation, a much lower (higher in the absolute value) segregation energy is found for the SP core (-0.62 eV) than for the DP core (-0.22 eV). For higher concentrations of 1 Fe atom/ξ, one can see that the segregation energy is significantly different for the 30° and 90° DP cores. For the SP core of the 90° dislocation, the segregation energy almost does not change.

In order to analyze how the thermodynamic stability of dislocation is affected by the segregation of impurity atoms, we computed the relative line energies for both clean and Fe-containing dislocations. For the clean dislocations, the relative line energy η_0 is calculated as

$$2\eta_0 = \frac{E^{\text{without Fe}} - E^{\text{ref}}}{4\xi}, \tag{3}$$

where the factor 2 accounts for the presence of two dislocations in our supercells. E^{ref} is an arbitrarily chosen reference energy. For the 30° dislocation, the natural reference is the energy of the clean dislocation so that $\eta_0 = 0$. For the 90° dislocations we chose the SP core energy as the reference so that the line energy of the more stable DP core is lower and negative. We can then determine the relative line energies of the Fe-decorated dislocation cores as

$$\eta = \frac{E^{\text{with Fe}} - N_{\text{Fe}}\mu_{\text{Fe}} - E^{\text{ref}}}{4\xi} - \eta_0. \tag{4}$$

This formula corrects for a double-counting contribution since in our supercells only one of the two dislocations is decorated with Fe atoms.

The results are summarized in Fig. 7 for both cores types. For the 30° core, the relative dislocation line energy is only weakly dependent on the concentration, with a marginal decrease at high concentration. For the 90° dislocations the concentration dependence is much more pronounced. It is close to linear in both cases and the relative line energies of both cores decrease significantly with increasing Fe concentration. Nevertheless, the relative thermodynamic

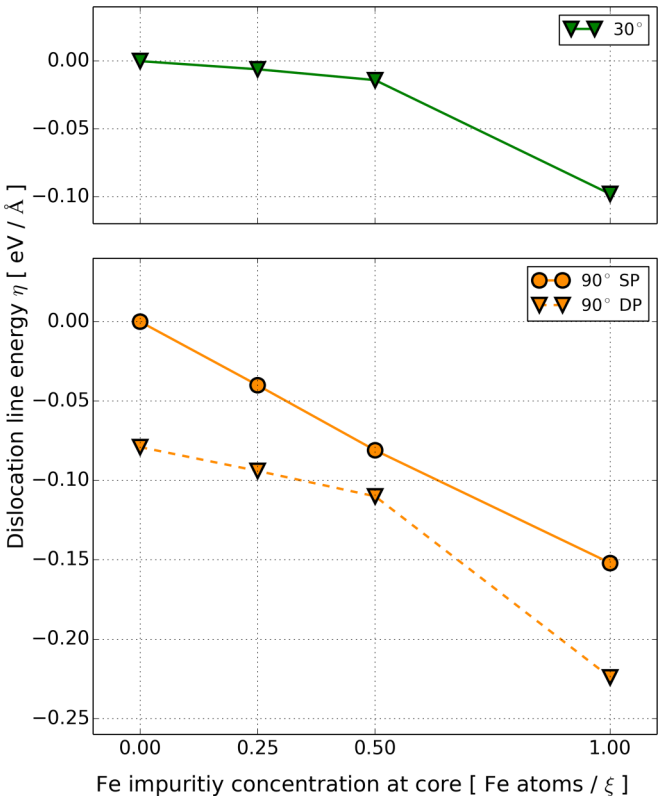

FIG. 7. (Color online) Relative dislocation line energy as a function of Fe impurity concentrations along the dislocation line.

stability of the reconstructed SP and DP cores remains unaltered, with the DP core being more stable at all Fe concentrations.

The electronic densities of states for an impurity concentration of 1 Fe atom/ξ reveal a formation of broader d bands that indicate chemical interaction between the Fe impurities. For the DP core of the 90° dislocation, the system becomes nonspin polarized. This behavior has been already observed in previous studies of segregated Fe impurities at large-angle grain boundaries [19]. It may indicate an initial stage of formation of the nonmagnetic β-$FeSi_2$ phase, but it is necessary to examine the relation between atomic structure, Fe concentration, and magnetic state in more detail to fully understand this transition. Our results show that large concentrations of Fe impurities at the dislocations are favored which implies that local clustering of Fe impurities at the dislocation line is possible even at low total Fe concentrations. Such clustering would again favor an iron-silicide nucleation.

Our findings for the Fe segregation at dislocation cores in Si are in accordance with experimental reports [4,5]. However, the segregation mechanism at the atomic scale is different than that expected by some of the experimental studies. For instance, Lauer *et al.* [4] assumed that the Fe interstitial binds to a dangling bond present in the core of a 60° dislocation, but this core structure is not energetically favorable [6]. Moreover, it is likely that dislocations in Si dissociate under normal conditions as it was observed using HRTEM by Reiche *et al.* [27]. Our results clearly show that Fe segregation at the dissociated dislocations is not only possible but also energetically favorable.

The electronic structure of Fe atoms segregated at dislocation cores is different from that of interstitial Fe impurities in bulk Si. For an individual Fe impurity at each of the considered dislocation cores, we can identify a Fe-related deep electronic defect level at about $E_V + 0.40$ eV (E_V stands for the highest energy of the valence band). This peak is located in the same energy range as the deep level for interstitial Fe in bulk Si [18,37–40]. Moreover, a second peak appears for all stable cores (90° DP and 30° dislocation core) which originates from the Fe d states and is located 0.42 eV higher in energy, i.e., at $E_V + 0.82$ eV. This peak may explain the metal-related deep level observed by deep-level transient spectroscopy (DLTS) at $E_V + (0.77 \pm 0.03)$ eV [41–43]. However, in these studies, the first deep level at $E_V + 0.40$ eV does not appear in the measured DLTS data. Another DLTS study by Lu *et al.* reported a deep level only at $E_V + 0.42$ eV but the deep level at $E_V + (0.77 \pm 0.03)$ eV was not observed [5]. Our calculations suggest that indeed both deep levels should be present. However, the electronic structure of Fe impurities at dislocation cores may be influenced by other conditions such as additional impurity elements, intrinsic defects at the dislocation line, etc.

Additional defects associated with dislocations, such as reconstruction defects [41] or vacancies at dislocation cores [44], have been reported previously. In bulk Si, interstitial Fe impurities interact readily with Si vacancies to form substitutional Fe defects [45]. Since vacancies are attracted by the dislocation cores, the formation of these defects is likely to be enhanced even more along dislocations, possibly leading to a preferential nucleation of iron silicides. The different chemical environments associated with a substitutional or interstitial Fe impurity interacting with an imperfect core reconstruction (i.e., a dangling bond) can also promote the formation of stronger Fe-Si bonds.

Another possible extension of this study is to consider also the interaction of interstitial Fe impurities with other point defects at the dislocation cores. For instance, Matsubara *et al.* showed that the local concentration of H at dislocations can be significantly increased and thus the formation of FeH pairs in the dislocations may become possible [12] and can affect the local electronic structure of the decorated dislocation. Some further impurity atoms have been shown to interact with dislocation, for instance, phosphorus [46], while other impurity atoms, in particular p-type dopants such as boron or gallium, are not attracted by partial dislocations [47].

Moreover, it is known that Fe impurities in Si change their charge states in the presence of dopants influencing the Fermi level. In further studies, it will become important to investigate the charge states of Fe impurities at the cores of dislocations using similar approaches as in Ref. [48].

To conclude, segregation of interstitial Fe impurities is possible at all cores of partial dislocations in Si. The segregation energy of Fe depends strongly on the type of dislocation but the core reconstruction is not affected by segregation of Fe for all considered impurity concentrations. In all cases additional electronic levels consisting of Fe d states are observed in the Si band gap which can give rise to an electrical activity of dislocations.

ACKNOWLEDGMENTS

This work was performed on the computational resource ForHLR Phase I funded by the Ministry of Science, Research and the Arts Baden-Württemberg and DFG ("Deutsche Forschungsgemeinschaft"). Atomistic structure models are visualized using VESTA [49]. This work was funded by the Hans L. Merkle Foundation of the Robert Bosch GmbH.

[1] M. Seibt, V. Kveder, W. Schröter, and O. Voß, Phys. Status Solidi A **202**, 911 (2005).
[2] J. Hofstetter, D. P. Fenning, D. M. Powell, A. E. Morishige, and T. Buonassisi, Solid State Phenom. **205-206**, 15 (2013).
[3] A. Istratov, T. Buonassisi, M. Pickett, M. Heuer, and E. Weber, Mater. Sci. Eng. B **134**, 282 (2006).
[4] K. Lauer, M. Herms, A. Grochocki, and J. Bollmann, Solid State Phenom. **178-179**, 211 (2011).
[5] J. Lu, X. Yu, Y. Park, and G. Rozgonyi, J. Appl. Phys. **105**, 073712 (2009).
[6] J. Rabier, L. Pizzagalli, and J. Demenet in *Dislocations in Solids*, edited by J. P. Hirth and L. Kubin (Elsevier, New York, 2010), Chap. 93, pp. 47–108.
[7] L. Pizzagalli, P. Beauchamp, and J. Rabier, Philos. Mag. **83**, 1191 (2003).
[8] C.-Z. Wang, J. Li, K.-M. Ho, and S. Yip, Appl. Phys. Lett. **89**, 051910 (2006).
[9] A. Valladares and A. P. Sutton, J. Phys.: Condens. Matter **17**, 7547 (2005).
[10] C.-y. Wang, Z.-q. Wang, Q.-y. Meng, C.-l. Li, and H.-w. Zheng, Superlattices Microstruct. **50**, 157 (2011).
[11] H. Zhang, Eur. Phys. J. B **81**, 179 (2011).
[12] M. Matsubara, J. Godet, and L. Pizzagalli, Phys. Rev. B **82**, 024107 (2010).
[13] M. Matsubara, J. Godet, and L. Pizzagalli, J. Phys.: Condens. Matter **22**, 035803 (2010).
[14] A. Antonelli, J. F. Justo, and A. Fazzio, J. Appl. Phys. **91**, 5892 (2002).
[15] A. Antonelli, J. F. Justo, and A. Fazzio, J. Phys.: Condens. Matter **14**, 12761 (2002).
[16] N. Fujita, R. Jones, S. Öberg, P. R. Briddon, and A. T. Blumenau, Solid State Phenom. **131-133**, 259 (2008).
[17] A. Istratov, H. Hieslmair, and E. Weber, Appl. Phys. A **69**, 13 (1999).
[18] M. Sanati, N. G. Szwacki, and S. K. Estreicher, Phys. Rev. B **76**, 125204 (2007).
[19] B. Ziebarth, M. Mrovec, C. Elsässer, and P. Gumbsch, Phys. Rev. B **91**, 035309 (2015).
[20] B. Ziebarth, M. Mrovec, C. Elsässer, and P. Gumbsch, Phys. Rev. B **92**, 115309 (2015).
[21] P. Giannozzi, S. Baroni, N. Bonini, M. Calandra, R. Car, C. Cavazzoni, D. Ceresoli, G. Chiarotti, M. Cococcioni, I. Dabo *et al.*, J. Phys.: Condens. Matter **21**, 395502 (2009).
[22] D. Vanderbilt, Phys. Rev. B **41**, 7892 (1990).
[23] J. P. Perdew, K. Burke, and M. Ernzerhof, Phys. Rev. Lett. **77**, 3865 (1996).
[24] S. R. Bahn and K. W. Jacobsen, Comput. Sci. Eng. **4**, 56 (2002).
[25] J. Hornstra, J. Phys. Chem. Solids **5**, 129 (1958).
[26] J. P. Hirth and J. Lothe, *Theory of Dislocations* (Krieger, Malabar, FL, 1991).
[27] M. Reiche, M. Kittler, W. Erfurth, E. Pippel, K. Sklarek, H. Blumtritt, A. Haehnel, and H. Uebensee, J. Appl. Phys. **115**, 194303 (2014).
[28] F. Liu, M. Mostoller, V. Milman, M. F. Chisholm, and T. Kaplan, Phys. Rev. B **51**, 17192 (1995).
[29] T. Kaplan, F. Liu, M. Mostoller, M. F. Chisholm, and V. Milman, Phys. Rev. B **61**, 1674 (2000).
[30] T.-L. Chan, D. West, and S. B. Zhang, Phys. Rev. Lett. **107**, 035503 (2011).
[31] E. Clouet, L. Ventelon, and F. Willaime, Phys. Rev. Lett. **102**, 055502 (2009).
[32] W. Cai, V. V. Bulatob, J. Chang, J. Li, and S. Yip, Philos. Mag. **83**, 539 (2003).
[33] J. R. Chelikowsky, Phys. Rev. Lett. **49**, 1569 (1982).
[34] J. Bennetto, R. W. Nunes, and D. Vanderbilt, Phys. Rev. Lett. **79**, 245 (1997).
[35] W. H. Press, *Numerical Recipes in Fortran 77: The Art of Scientific Computing* (Cambridge University Press, Cambridge, 1992), Vol. 1.
[36] See Supplemental Material at http://link.aps.org/supplemental/10.1103/PhysRevB.92.195308 for some further configurations of Fe atoms at dislocation cores in silicon which are higher in energy than the ones that are discussed here.
[37] K. Wünstel and P. Wagner, Appl. Phys. A **27**, 207 (1982).
[38] K. Nakashima and M. Chijiiwa, Jpn. J. Appl. Phys. **25**, 234 (1986).
[39] O. O. Awadelkarim and B. Monemar, J. Appl. Phys. **64**, 6306 (1988).
[40] A. Rohatgi, J. R. Davis, R. H. Hopkins, P. Rai-Choudhury, P. G. McMullin, and J. R. McCormick, Solid-State Electron. **23**, 415 (1980).
[41] M. Seibt, R. Khalil, V. Kveder, and W. Schröter, Appl. Phys. A **96**, 235 (2009).
[42] V. Kveder, V. I. Orlov, M. Khorosheva, and M. Seibt, Solid State Phenom. **131-133**, 175 (2008).
[43] A. Castaldini, D. Cavalcoli, A. Cavallini, and S. Pizzini, Phys. Rev. Lett. **95**, 076401 (2005).
[44] J. F. Justo, M. de Koning, W. Cai, and V. V. Bulatov, Phys. Rev. Lett. **84**, 2172 (2000).
[45] S. K. Estreicher, M. Sanati, and N. Gonzalez Szwacki, Phys. Rev. B **77**, 125214 (2008).
[46] Y. Ohno, T. Shirakawa, T. Taishi, and I. Yonenaga, Appl. Phys. Lett. **95**, 091915 (2009).
[47] Y. Ohno, Y. Tokumoto, H. Taneichi, I. Yonenaga, K. Togase, and S. R. Nishitani, Physica B **407**, 3006 (2012).
[48] C. Freysoldt, B. Grabowski, T. Hickel, J. Neugebauer, G. Kresse, A. Janotti, and C. G. Van de Walle, Rev. Mod. Phys. **86**, 253 (2014).
[49] K. Momma and F. Izumi, J. Appl. Crystallogr. **44**, 1272 (2011).